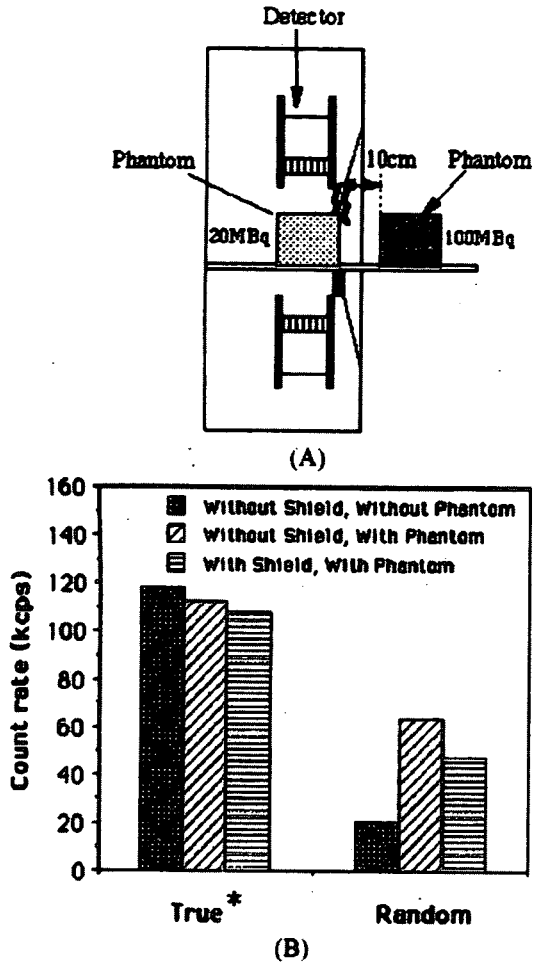

Fig. 5. Experimental set-up of phantoms positioned in FOV and out-of-FOV (A), true* ((B)-left), and random ((B)-right) count rates with and without the curtain-shield.

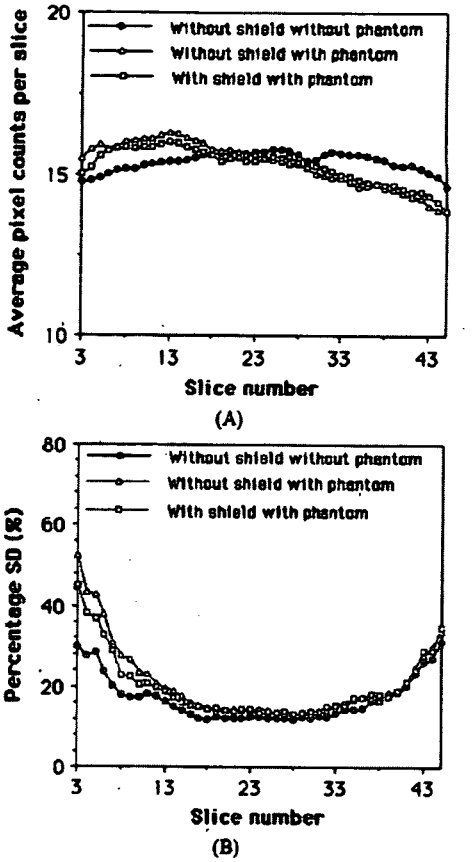

Fig. 6. Average pixel counts (A) and %SD (B) for each slice with phantom of 20 MBq in the FOV and another phantom of 100 MBq with and without positioned out-of-FOV.

Next, we measured the prompt minus delay and random rates with two 20 cm diameter, 20 cm long phantoms. One, containing 20 MBq, was placed in the scanning field, and another, containing 100 MBq, was placed 10 cm from the edge of the FOV. The phantom arrangement of this experiment is shown in Fig. 5(A). This measurement was intended to simulate human body study in which the large amount of radioactivity exists out-of-FOV. Measurements were made with and without the curtain-shield.

Results are shown in Fig. 5. In this figure, true* is the prompt minus delay rate, which is equivalent to the true plus scatter rate. Using the curtain-shield, true* rate slightly decreased probably because of the decrease of the scatter from the out-of-FOV phantom. The random rate decreased 25% by using the curtain-shield. In this experiment, true* rates decreased with the out-of-FOV phantom both with and without the curtain-shield. This probably reflects the deadtime from the out-of-field activity.

We measured the reconstructed pixel value and percentage standard deviation (%SD) of the same set-up as the previous experiment (phantom of 20 MBq in the FOV of the PET scanner and another phantom of 100 MBq positioned out-of-FOV). Neither scatter correction nor deadtime correction were applied for the reconstruction images. Fig. 6 shows average pixel counts and %SD for each slice. For slices 3–20 (farthest slices from the out-of-FOV activity), both average pixel counts and %SD increased with the out-of-FOV phantom.

The asymmetry of the slice sensitivity (average pixel counts) came from the scatter events from out-of-FOV activity; i.e., the slices (detector rings) closer to the out-of-FOV phantom were shaded by the internal fixed-shield of the PET scanner from the scatter events produced in the out-of-FOV phantom, while the slices (detector rings) farthest from the phantom were not effectively shaded. Also the decrease of the average counts in higher slices (~30–45: closer to the curtain-shield) with out-of-FOV phantom probably came from the increase of the singles deadtime. Using curtain-shield, the both average pixel counts and %SD slightly decreased meaning that scatter and random decreased.

B. Human Studies

To show the effectiveness of the curtain-shield in clinical situations, we measured the prompt minus delay (true*), random, and noise equivalent count (NEC) rates for FDG human volunteer studies (3D-acquisition mode). The true* in this measurement contains scatter because the scatter contribution is difficult

TABLE I
TRUE*, RANDOM, AND NEC RATES FOR FDG HUMAN STUDIES WITH AND WITHOUT THE CURTAIN-SHIELD FOR CHEST AND ABDOMINAL REGIONS

Region	Chest			Abdominal		
	True*	Random	NEC	True*	Random	NEC
Without shield	107 kcps	70.6 kcps	46.1 kcps	84.8 kcps	71.4 kcps	31.5 kcps
With shield	107 kcps	57.0 kcps	51.8 kcps	85.0k cps	59.4 kcps	35.5 kcps

to estimate and separate from the true*. The NEC rate is calculated by the following equation:

$$\text{NEC rate} = (\text{true}^*)^2/(\text{true}^* + 2 \text{ x random}).$$

This calculation overestimates the NEC rate for both without and with shield conditions because scatter is not included in the calculation and the true* contains scatter.

A subject was injected with 200 MBq of FDG. Measurements were started 50 min after injection. Measurements were made for the chest and abdominal regions, which are respectively affected by FDG accumulation in the brain and bladder.

Table I shows the true*, random, and NEC rates for FDG human studies with and without the curtain-shield. In the FDG studies in both chest and abdominal region imaging, random rates decreased approximately 20%. NEC rates increased 12% for the chest region and 13% for the abdominal region.

IV. DISCUSSION AND CONCLUSION

We developed and tested a curtain-shield. Because it is flexible, it could be used safely even in body studies.

In the experiments, the curtain-shield was only attached to the front region of the PET scanner. It can also be used on the back of the PET scanner. By using the curtain-shield on both sides of the PET scanner, the effectiveness (reduction of random and scatter) will be increased more although it is difficult to hang the shield at the back end of the detector ring.

For obese subjects, the curtain-shield might touch them and could be dragged into the scanner. This might decrease the sensitivity of the slices near the curtain-shield and may cause artifacts in the images. To avoid these problems, a solution is to reduce the length of the curtain-shield by folding it up at the joints of the tungsten plates before scanning because the joints of the curtain shield are flexible and easy to fold.

In Fig. 6(A), asymmetry distribution of the slice sensitivity (pixel counts) with out-of-FOV phantom was significant without scatter and deadtime corrections. Precise corrections are needed to correct the asymmetry distribution. The curtain-shield can improve the asymmetry distribution although the impact is not large.

Contributions from scatter and random events from out-of-FOV will be more serious for new PET scanners with longer axial FOV [7] and for PET/CT scanners with larger patient ports [8], [9]. In these PET systems, the developed curtain-shield will be more effective in random and scatter rejection.

ACKNOWLEDGMENT

The authors would like to thank the Matsuki Co. for manufacturing some parts of the curtain-shield.

REFERENCES

[1] S. Yamamoto, S. Miura, Y. Shouji, H. Iida, and I. Kanno, "Development of a front shield for a 3D positron emission tomography," *Kaku Igaku*, vol. 33, no. 6, pp. 641–646, 1996.

[2] T. J. Spinks, M. P. Miller, D. L. Bailey, P. M. Bloomfield, L. Livieratos, and T. Jones, "The effect of activity outside the direct field of view in a 3D-only whole-body positron tomography," *Phys. Med. Biol.*, vol. 43, no. 4, pp. 895–904, 1998.

[3] C. J. Thompson, S. Kecani, and S. Boelen, "Evaluation of a neck-shield for use during neurological studies with a whole-body PET scanner," *IEEE Trans. Nucl. Sci.*, vol. 48, no. 4, pp. 1512–1517, 2001.

[4] M. E. Daube Witherspoon, A. Belakhlef, S. L. Green, and I. Zanzi, "Design of patient shielding to reduce the effect of out-of-field radioactivity in 3D PET," in *IEEE Nuclear Science Symp., Conf. Rec.*, 1998, vol. 2, pp. 1237–1242.

[5] R. Boellaard, H. W. de Jong, C. F. Molthoff, F. Buijs, M. Lenox, R. Nutt, and A. A. Lammertsma, "Use of an in-field-of-view shield to improve count rate performance of the single crystal layer high-resolution research tomograph PET scanner for small animal brain scans.," *Phys. Med. Biol.*, vol. 48, no. 23, pp. N335–42, 2003.

[6] T. Hasegawa, H. Murayama, H. Matsuura, T. Yamaya, and S. Tanada, "Shielding effects of body-shields for 3D PET," *Igaku Butsuri.*, vol. 22, no. 4, pp. 318–326, 2002.

[7] S. Surti and J. S. Karp, "Imaging characteristics of a 3-dimensional GSO whole-body PET camera," *J. Nucl. Med.*, vol. 45, no. 6, pp. 1040–1049, 2004.

[8] O. Mawlawi, D. A. Podoloff, S. Kohlmyer, J. J. Williams, C. W. Stearns, R. F. Culp, and H. Macapinlac, "Performance characteristics of a newly developed PET/CT scanner using NEMA standards in 2D and 3D mode," *J. Nucl. Med.*, vol. 45, no. 10, pp. 1734–1742, 2004.

[9] Y. E. Erdi, S. A. Nehmeh, T. Mulnix, J. L. Humm, and C. C. Watson, "PET performance measurements for an LSO-based combined PET/CT scanner using the National Electrical Manufacturers Association NU 2-2001 standard," *J. Nucl. Med.*, vol. 45, no. 5, pp. 813–21, 2004.

原著

二次元および三次元PET収集における雑音等価計数と再構成画像の画質の評価

松本圭一[1,2]・清水敬二[1]・北村圭司[3]
渡辺英治[1]・村瀬研也[2]・千田道雄[1]

1)先端医療センター分子イメージンググループ
2)大阪大学大学院医学系研究科保健学専攻医用物理工学講座
3)株式会社島津製作所医用機器事業部技術部

論文受付
2006年4月12日
論文受理
2006年6月22日
Code Nos. 333
523

緒言

陽電子放出断層撮影装置(PET装置)にて計測される即発同時計数には，画像を構築する真の同時計数以外に偶発同時計数と散乱同時計数が含まれる．後者二つの計数は定量性だけでなく画質にも大きく影響するため，補正(減算)を行い定量性の高いPET画像を作成している．PET装置における画質評価は，受診者動作特性曲線を用いた観察者視覚評価もしばしば行われるが[1,2]，計数率から簡便に画質を推測できる雑音等価計数(noise equivalent count；NEC)[3,4]の方が広く用いられている．NECは偶発同時計数と散乱同時計数を考慮したPET計測における信号雑音(signal/noise；S/N)比の指標であり，次式で表される．

$$NEC = \frac{T^2}{T + S + (1+k)fR} \quad \cdots\cdots(1)$$

ここで，Tは真の同時計数，Sは散乱同時計数，Rは

Comparison of Noise Equivalent Count Rate and Image Quality for Two-dimensional and Three-dimensional PET Scans

Keiichi Matsumoto,[1,2] Keiji Shimizu,[1] Keishi Kitamura,[3] Eiji Watanabe,[1] Kenya Murase,[2] and Michio Senda[1]

1)Division of Molecular Imaging, Department of Image-based Medicine, Institute of Biomedical Research and Innovation
2)Department of Medical Physics and Engineering, Division of Medical Technology and Science, Course of Health Science, Graduate School of Medicine, Osaka University
3)R&D Department, Medical Systems Division, Shimadzu Corporation

Received April 12, 2006; Revision accepted June 22, 2006; Code Nos. 333, 523

Summary

The aim of this study was to investigate the correlation between noise equivalent count(NEC)rates and the signal-to-noise ratio(S/N)in reconstructed images. The NEC rates were determined using uniform 20 cm and 70 cm tall, 20 cm diameter cylinders filled with ^{11}C. The phantoms were scanned in both two-dimensional and three-dimensional modes. The reconstructed image noise was evaluated using FBP and OSEM algorithms(4 iterations and 8 subsets). The images were filtered to a final image resolution of 6.5 mm. From the reconstructed image sets, averages and standard deviations of images were generated, from which the average image S/N(=average/standard deviation)was calculated within an 18 cm central ROI. The S/N of a central slice and an end slice was compared with the NEC. The NEC was found to have a linear relationship to the image S/N of all slices, depending on differences in noise properties specific to the reconstruction algorithm. In two-dimensional mode, although the image S/N of the central slice and the edge slice showed a linear relationship with the NEC, in three-dimensional mode, the S/N of the central slice did not show a relationship with the NEC. The linear relationship was also found in both two- and three-dimensional acquisition modes, as well as for the different activity distributions. These results indicate that the NEC is not only a measure for comparing the count rate performance of imaging systems. However, an absolute evaluation is impossible to depend on reconstruction algorithm, slice number, and phantom type.

Key words: positron emission tomography (PET), noise equivalent count (NEC), image quality, filtered back projection (FBP), ordered subsets expectation maximization (OSEM)

別刷資料請求先：〒650-0047 神戸市中央区港島南町2丁目2番
先端医療センター 分子イメージンググループ 松本圭一 宛

偶発同時計数，fは被写体(ファントム)が断面内の有効視野内に占める割合である．kは偶発同時計数の補正方法に依存する係数であり，遅延同時計数回路により偶発同時計数を実測する場合は1となる．NECは偶発および散乱同時計数補正が適切に施されていることを前提とした指標であるが，計数率から簡便にS/N比を推測できるため物理学的性能評価[4]や全身検査の投与量決定[5]などに用いられている．

一方，近年のPET装置は感度を向上させるために，体軸方向視野の拡大や三次元収集を行って検出器受容立体角(幾何学的効率)を拡大させている．セプタを使用しない三次元収集は，視野全体の感度を飛躍的に向上させることが可能であるが，検出器最大リング差や体軸方向のline of responseの束ね(span)に依存して中央スライスよりも両端スライスの感度(計数率)が低下する[6]．加えて三次元収集は，視野外放射線が偶発および散乱同時計数となって定量性や画質を劣化させることが報告されている[7]．これは，偶発同時計数が一般に遅延同時計数回路によって補正されるためであり，(1)式分母における偶発同時計数の増加($2R$)にて説明できる．また市販のPET装置に広く標準装備されているシミュレーションベースの散乱補正法[8]は，厳密には視野外放射線による散乱同時計数に対応していないため，視野外放射線が多くなるほど定量性や画質の劣化が顕著になる．

NECを用いてS/N比を評価するためには，収集方法，視野外放射線さらには画像再構成法に依存することなく，低放射能濃度から高放射能濃度まで直線(相関)性が担保されている必要がある．加えて，視野全体の計数率からS/N比を推測するNECが，各画像スライスのS/N比と相関関係にあれば，さまざまな条件下における画質評価に用いることができると考えられる．本研究の目的は，収集方法，視野外放射線，放射能濃度および画像再構成法を変化させて，NECとPET画像のS/N比の関係を評価することである．

1．方　法

1-1　使用機器および測定方法

使用したPET装置はECAT EXACT HR+[9](SIEMENS社製)で，検出器リング間を隔てるセプタを出し入れすることで二次元および三次元収集が可能である．セプタの素材はタングステンであり，長さ66.5mm，厚み0.8mmである．4.39×4.05×30mmのBGO結晶を総計18,432個有し，スライス間隔2.4mmにて63画像スライス(32検出器リング)を撮像可能である．体軸方向の有効視野は15.5cmであり，視野中心における断面方向および体軸方向の空間分解能は，二次元収集がそれぞれ4.5mmと4.9mmであり，三次元収集は4.3mmと4.1mmである[9]．またエネルギーウィンド設定は350～650keVであり，トランスミッション用外部線源として^{68}Ge-^{68}Ga(initial activity：185MBq/本)線線源を3本有している．検出器最大リング差とspanは，二次元収集がそれぞれ7と15であり，三次元収集は22と9である．

PET測定は，^{11}C溶液を封入した20cmϕ×20cm(6283.2cm^3)と20cmϕ×70cm(21991.2cm^3)の円筒ファントムを用いた．PET装置の性能評価のための測定指針[10]に準拠して，高計数率特性(計数損失等の補正と精度とS/Nの比)の測定を二次元と三次元収集で行った．指針では，「計数損失および偶発同時計数が無視できるような計数率まで測定し，測定間隔は使用核種の半減期の1/2以下，かつ各フレームの測定時間は半減期の1/4以下とし，全体の測定は5半減期以上にわたってダイナミック測定を行う」としている．本研究ではファントム封入用に^{11}C溶液(半減期：20.4min)を封入したため，測定間隔および各フレームの測定時間を5分とした30フレームのダイナミック測定を行い，全体の測定時間は約5時間とした．二次元収集における測定開始時間でのファントム内放射能濃度は，20cmϕ×20cmファントムが757.1kBq/mlであり，20cmϕ×70cmファントムが357.0kBq/mlである．同じく三次元収集では，20cmϕ×20cmファントムが206.3kBq/mlであり，20cmϕ×70cmファントムが145.6kBq/mlである．またトランスミッション測定はファントム内に放射能がない状態で30分間測定した．

1-2　データ処理

すべての測定データは，計数損失補正，偶発同時計数補正(delayed coincidence correction)，散乱線補正(2D：deconvolution method[11]，3D：single scatter simulation algorithm[8])，および吸収補正を行った後，filtered back projection(FBP)法とordered subsets expectation maximization(OSEM)法を用いて画像再構成を行った．OSEM法における繰り返し回数とサブセット数は，臨床条件と同様にそれぞれ4と8を選択した[12]．平滑化フィルタにはGaussianフィルタ(6mm FWHM)を使用し，マトリックスサイズは128×128，ボクセルサイズは2.6×2.6×2.4mmとした．また，三次元収集されたエミッションデータは，Fourier rebinning法[13]にて近似的に二次元データに変換した．

1-3　データ解析

1-3-1　NECの算出

PET画像は即発同時計数から偶発同時計数と散乱同時計数を補正して画像を作成するため，それらが全くない理想的な場合の画像と比較してS/N比は低下す

Table Reported JIRA 1994 performance characteristics for PET scanner.

	2-dimensional	3-dimensional
Scatter fraction of System (%)	19	37

る．NECは，それらS/N比を劣化させる計数率を考慮して画質を推測する指標である．

2種類の異なるファントムにおける二次元および三次元収集のNECは(1)式を用いて算出した．偶発同時計数は遅延回路により実測した値を用いたため，(1)式におけるkを1とした．断面内の有効視野が65.3cmであるためファントムが占める割合(γ)は0.31とし，真の同時計数は次式を用いて算出した．

$$T=(T+S)\times(1-scatter\ fraction) \quad \cdots\cdots(2)$$

散乱フラクションは，均一な放射能濃度を持つ円筒ファントムに対する散乱同時計数の割合である．PET装置の性能評価のための測定指針[10, 14]に準拠して20cmϕ×20cmファントムを用いてあらかじめ測定した値を用いた(Table)．

1-3-2 PET画像のS/N比

各フレームにおける各画像スライスの中心に18cmの円形関心領域を設定し，その画像放射能濃度の平均値と標準偏差から次式を用いてPET画像のS/N比を算出した．

$$Image\ noise(S/N)^2=\left(\frac{average}{standard\ deviation}\right)^2 \quad \cdots\cdots(3)$$

本研究では，全63画像スライスの平均S/N比のほかに，中央10スライスと両端5スライス(計10スライス)の平均S/N比も算出し，それぞれ最大NECまでの計数率と比較を行った．加えて，最大NECにおける各スライスのS/N比を比較した．

2．結　果

二次元および三次元収集における各ファントムのNECをFig. 1とFig. 2に示す．二次元収集におけるNECは，両ファントムともに30kBq/ml以上の放射能濃度から緩やかに低下したが(Fig. 1)，三次元収集におけるNECは，20cmϕ×20cmファントムでは約12kBq/ml以上で，20cmϕ×70cmファントムでは約6kBq/ml以上の放射能濃度で急激に低下した(Fig. 2)．20cmϕ×20cmファントムおよび20cmϕ×70cmファントムにおける最大NEC(放射能濃度)は，二次元収集でそれぞれ29.4kcps(45.9kBq/ml)と11.3kcps(21.6kBq/ml)であり，三次元収集では79.2kcps(12.5kBq/ml)と27.3kcps(6.3kBq/ml)であった．また両収集ともに20cmϕ×70cmファントムの方がすべての放射能濃度でNECが低値であった．

二次元収集におけるNECとS/N比の関係をFig. 3とFig. 4に示す．直線は全63画像スライスの平均S/N比における回帰曲線である．20cmϕ×20cmファントムおよび20cmϕ×70cmファントムともにNECとPET画像のS/N比はほぼ比例(直線)関係を示したが，最大NEC付近では直線関係を示さなかった．また20cmϕ×70cmファントムにおけるFBP法のS/N比が最も低値であった．FBP法およびOSEM法ともにNECが高値になるほど，中央スライスと両端スライスのS/N比に差を認めた．また両ファントムとも，すべてのNECでOSEM法のS/N比が高値であり，20cmϕ×70cmファントムではその差が顕著であった．

三次元収集におけるNECとS/N比の関係をFig. 5とFig. 6に示す．Fig. 3およびFig. 4と同様に，直線は全63画像スライスの平均S/N比における回帰曲線である．三次元収集においても，二次元収集と同様に最大NEC付近でS/N比のバラツキが大きかった．FBP法における全63画像スライスのS/N比は，両ファントムともにNECと良好な直線関係を示したが，中央スライスのS/N比は直線性が不良であった．またOSEM法においては，両ファントムとも両端スライスのS/N比以外は直線関係が不良であり，中央スライスのS/N比は10kcps以上のNECで直線性が不良であった．

Fig. 7に最大NECにおけるFBP法の各スライスのS/N比を示す．二次元収集における20cmϕ×70cmファントムのS/N比が最も低値であった．また三次元収集では，収集の物理的特性および視野外放射線の影響を受けて，両端スライスのS/N比が低下する傾向にあった．

3．考　察

NECは放射能分布が均一ファントムを用いて画質を推測できるため汎用されている．しかしながら，使用するファントムの長さ(視野外放射線)や大きさ，さらには収集方法に依存して偶発同時計数や散乱同時計数が異なり[15]，加えて再構成法(再構成パラメータ)に依存して画質が異なるため[16]，NECと画質に相関性を示すかは不明である．一方，計測学において統計雑音すなわち標準偏差を正確に評価するためには同一条件化で複数回の測定が必要であるが[17]，PET計測においては非常に難しい測定となる．そこで本研究では，関心領域内の画素値の標準偏差がPET画像の統計雑音に比

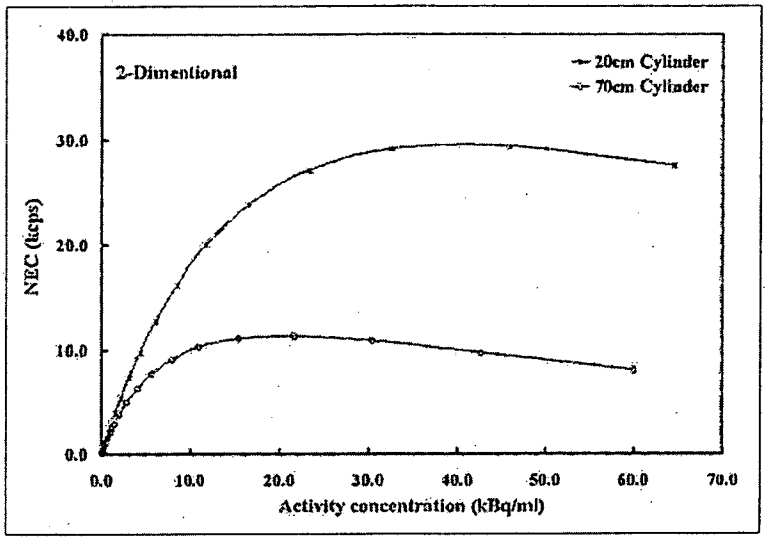

Fig. 1 NEC for the 20 cm and 70 cm tall cylinders, acquired in two-dimensional mode.

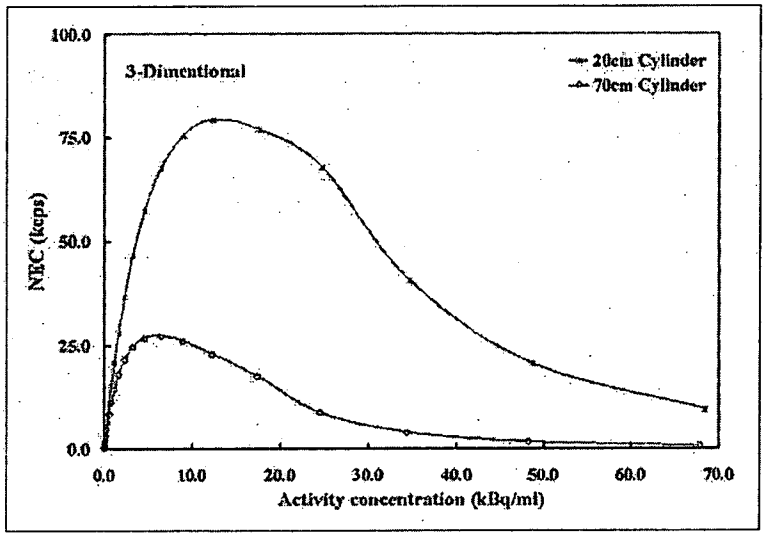

Fig. 2 NEC for the 20 cm and 70 cm tall cylinders, acquired in three-dimensional mode.

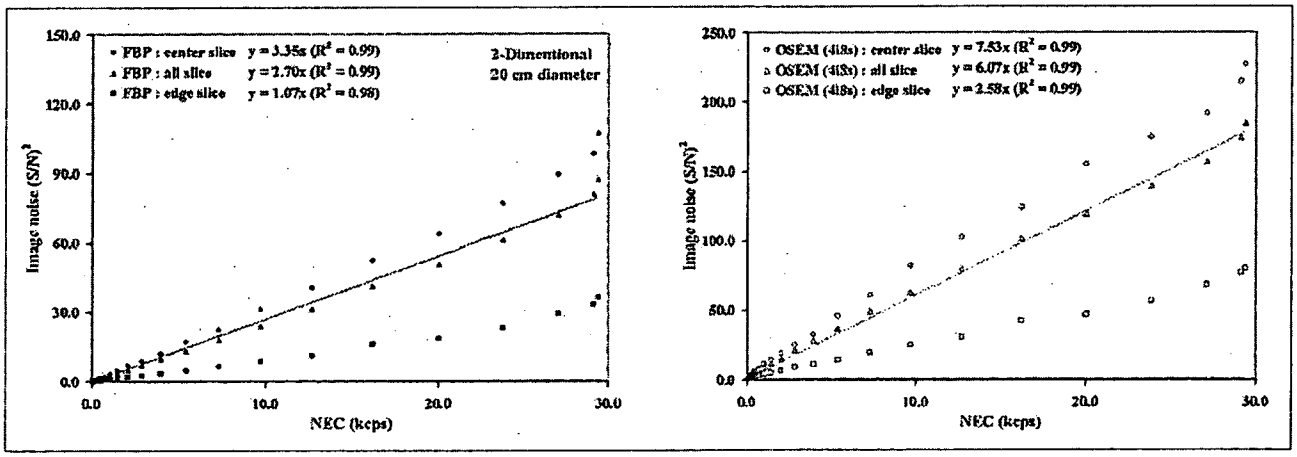

Fig. 3 Corresponding image noise $(S/N)^2$ plotted against NEC for 20 cm tall cylinders, where the image reconstructed FBP (a) and OSEM $4i8s$ (b), acquired in two-dimensional mode. Data points of all slices approach a straight line.

a | b

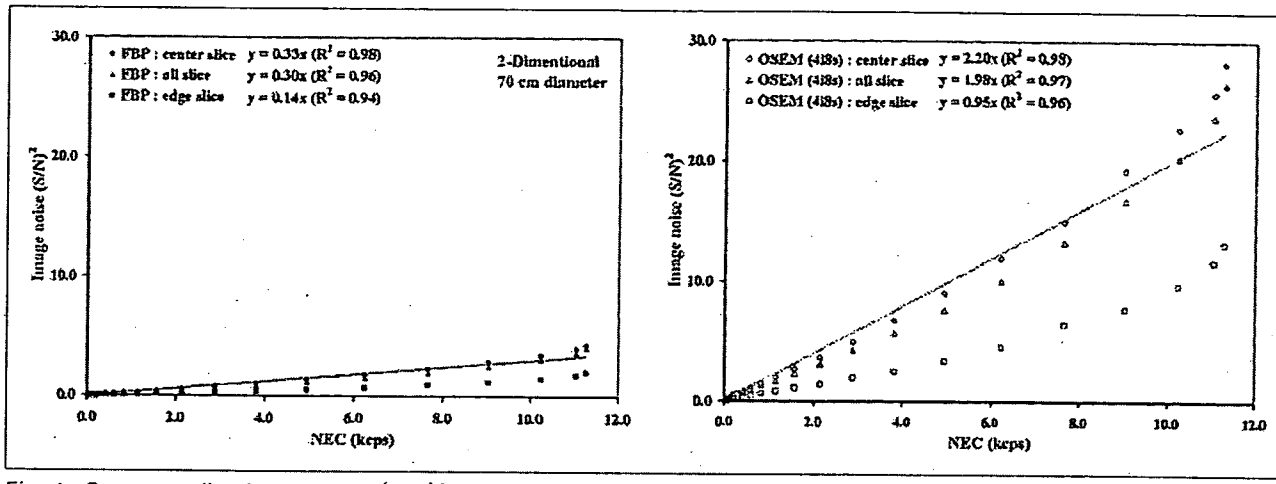

Fig. 4 Corresponding image noise $(S/N)^2$ plotted against NEC for 70 cm tall cylinders, where the image reconstructed FBP (a) and OSEM $4i8s$ (b), acquired in two-dimensional mode. Data points of all slices approach a straight line.

a | b

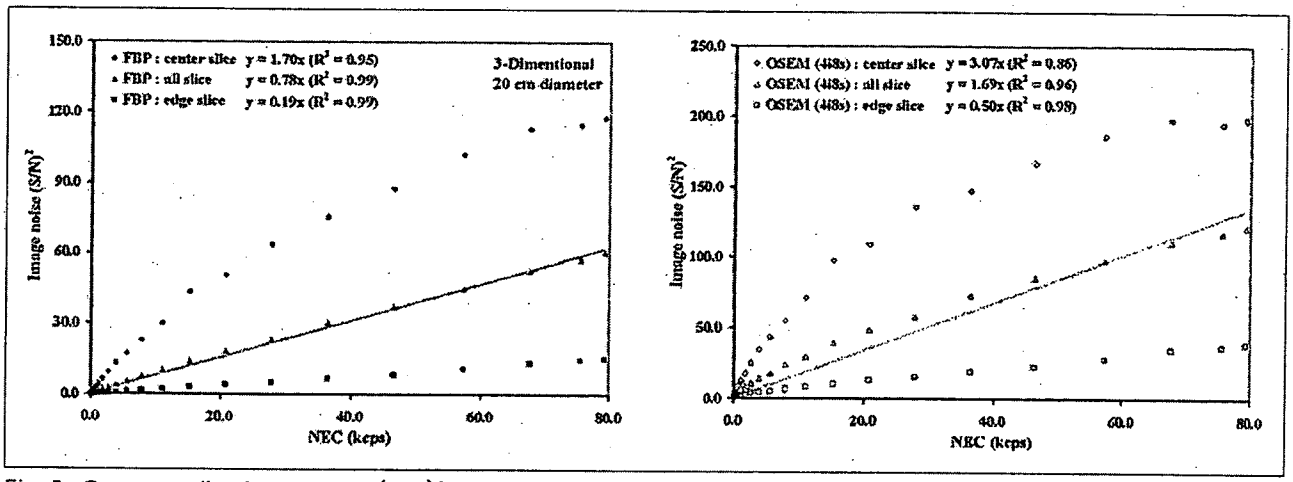

Fig. 5 Corresponding image noise $(S/N)^2$ plotted against NEC for 20 cm tall cylinders, where the image reconstructed FBP (a) and OSEM $4i8s$ (b), acquired in three-dimensional mode. Data points of all slices approach a straight line.

a | b

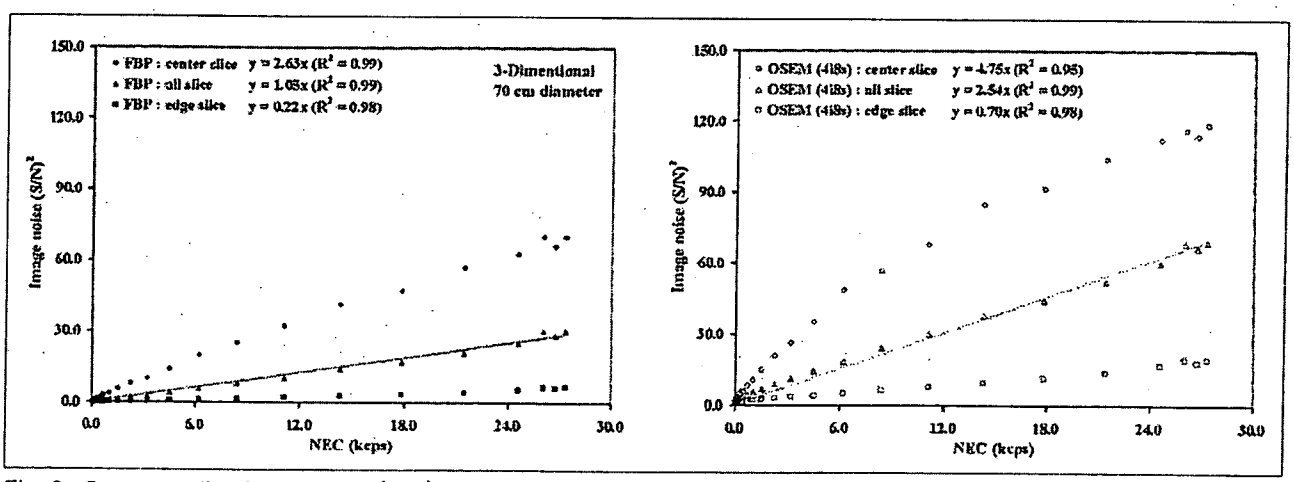

Fig. 6 Corresponding image noise $(S/N)^2$ plotted against NEC for 70 cm tall cylinders, where the image reconstructed FBP (a) and OSEM $4i8s$ (b), acquired in three-dimensional mode. Data points of all slices approach a straight line.

a | b

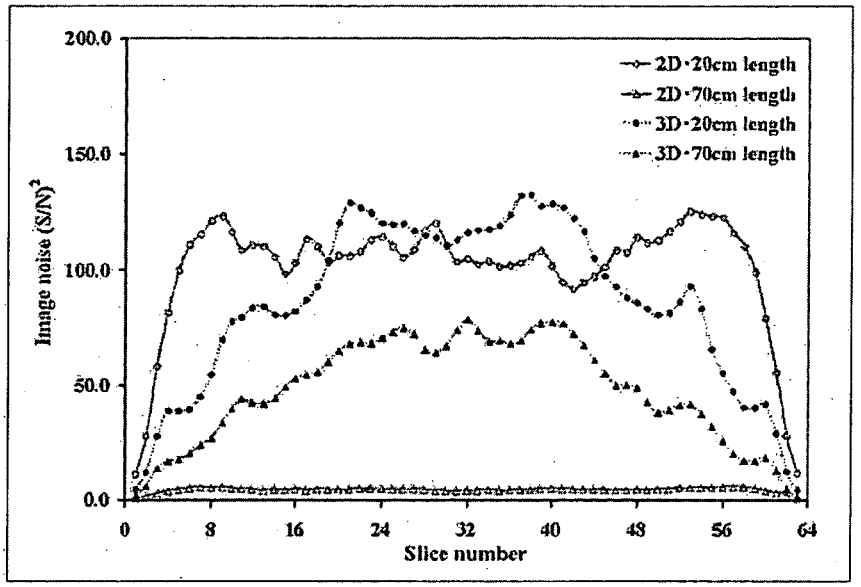

Fig. 7 Comparison of image noise for peak NEC acquired in two- and three-dimensional mode. All images were reconstructed by FBP.

例すると仮定し，さまざまな条件下でNECとPET画像のS/N比を評価した．

三次元収集のNECだけでなく，二次元収集におけるNECも視野外放射線の影響を強く受けた(Fig. 1，2)．二次元収集であっても視野外放射線が存在する場合には，PET装置のセプタ厚や，各検出器とファントムとの幾何学的効率に依存して偶発同時計数は増加する．言い換えると，視野外放射線が存在しない場合に真の同時計数として計測される事象も，視野外放射線の存在によって偶発同時計数として計測されてしまい，偶発同時計数の増加だけでなく真の同時計数の減少をきたす．二次元収集の利点は散乱および偶発同時計数が少ないことであるが，欠点として真の同時計数も少ない．このため視野外放射線の存在に起因する真の同時計数の減少がNECに大きく影響したと考えられる．

三次元収集において，20cmϕ×20cmファントムでは約7kBq/ml以上で，20cmϕ×70cmファントムでは約13kBq/ml以上の放射能濃度でNECの低下を認めた(Fig. 2)．これは偶発同時計数と散乱同時計数の増加およびそれに伴うPET装置と収集コンピュータにおけるデータ転送の飽和が原因であると考えられる．データ転送の飽和は，検出器の種類や信号処理回路などに依存するが，高いNECを獲得する放射能の濃度幅が小さいため臨床検査においては投与放射能量の最適化が非常に重要であると考える．しかしながら，ファントム実験(20cmϕ×70cmファントム)にて最大NECを得る放射能濃度は人体における最適投与量とならない[5, 18]．これは被検者の放射能分布や散乱体が一様でないためであり，使用核種，体内分布および撮像部位を考慮すれば，より低い放射能濃度が人体における最適投与量になると考える．

二次元収集における20cmϕ×20cmファントムのS/N比は，両画像再構成法とも広い範囲で良好な直線関係を示した(Fig. 3)．またPET収集の物理特性を反映して中央スライスは高いS/N比を，両端スライスは低いS/N比を示した．しかしながら，その直線性は最大値NECの90％程度までであり，最大NEC付近ではすべての条件において(Fig. 3～6)バラツキを認めた．これは高放射能濃度におけるパルスパイルアップ現象[19]のためと考える．すなわち，二つ以上のγ線が一つのブロック検出器にほぼ同時に入射して，検出器(光電子増倍管)の信号パルスが重なり合い，位置やエネルギー情報のミスコーディングを生じて最終的に検出器の感度ムラをきたしたと考えられる．また，FBP法におけるS/N比がOSEM法と比較して約1/2倍低値を示したのは，画素値に負の値を有しているためバラツキ(標準偏差)が大きくなったことが原因と考えられ，画像再構成法の特徴を表した結果であると考える[20]．一方，20cmϕ×70cmファントムのS/N比は，前述の結果(Fig. 3)と同様に最大NECの90％程度まで直線性を認めたが，FBP法では顕著にS/N比が低値であった(Fig. 4a)．NECが10kcps未満(Fig. 1)，すなわち低計数率では逐次近似画像再構成法(OSEM法)が有用であると考えられた．また，二次元収集におけるNECと全63画像スライスおよび中央スライスのS/N比は，ほぼ同等の傾きを保つ回帰式で表すことが可能であった．これは二

次元収集における視野内の真の同時計数が比較的均等に各スライスに分配されるためであり，各画像スライスのS/N比が広い範囲で均一であったことからも説明できる(Fig. 7)．したがって，二次元収集ではNECを用いて全画像スライスのS/N比および中央スライスのS/N比を推測可能であると考える．

三次元収集における両ファントムの全63画像スライスおよび両端スライスのS/N比は，二次元収集と同様に最大NECの90％程度まで良好な直線関係を示したが，中央スライスのS/N比のみ直線性が不良であった(Fig. 5, 6)．三次元収集は収集の特性上，視野外放射線源の有無にかかわらず中央スライスの計数率，すなわち真の同時計数と偶発同時計数が両端スライスよりも高くなる．本研究で使用した偶発同時計数補正は，即発同時計数からリアルタイムに差し引く方法であり，差分によって真の同時計数の統計ノイズが増大する特徴を有している．このため，高NECでは多くの偶発同時計数を減算することになり，結果としてNECとS/N比が直線関係を示さなかったと考える．高NECすなわち偶発同時計数が多い場合には，遅延同時計数を別の収集メモリに収集しておき，測定終了後に適当な平滑化処理やノイズ低減処理を施したのち減算処理を行う方法[21]が有効であると考えられた．また三次元収集におけるNECは，前述の理由から全画像スライスの平均的なS/N比を推測していると考えられた．

高いS/N比のPET計測を行うためには，PET装置の感度や投与量を増加させることが一般的であるが，(1)式に示すようにTの増加をSやRの増加で相殺せぬようにPET計測しなければならない．散乱同時計数は被写体の大きさ(断面積)に依存するが，視野外放射線が存在する場合には正確に偶発同時計数と分離することは不可能であるため散乱フラクションは大きくなる[22]．偶発同時計数補正によるノイズの増加を抑制することも重要であるが，視野外放射線を考慮した新しい散乱補正法[23]を適用することでさらに画質は向上すると考える．NECは真の同時計数，偶発同時計数および散乱同時計数を考慮したPET計測における有効な画質推測指標である．しかしながら，偶発および散乱同時計数補正の精度およびPET収集のスライス感度特性に影響することに十分注意する必要がある．

4．結　語

収集方法および視野外放射線を変化させて，NECから画質を評価できるか検討を行った．二次元および三次元収集におけるNECは，全画像スライスの平均的な画質を評価する指標であった．また，視野外放射線の影響すなわち偶発同時計数の増加は画質と密接な関係にあるため補正方法の選択が重要であると考えられた．加えて三次元収集における中央スライスのS/N比はNECと直線関係を示さないため，NECを用いた画質評価は注意が必要であると考えられた．

本論文の要旨は第45回日本核医学学会総会(2005年11月，東京)にて発表した．

参考文献

1) Glatting G, Werner C, Reske SN, et al.: ROC analysis for assessment of lesion detection performance in 3D PET: influence of reconstruction algorithms. Med Phys, 30(9), 2315-2319,(2003).
2) Farquhar TH, Llacer J, Sayre J, et al.: ROC and LROC analyses of the effects of lesion contrast, size, and signal-to-noise ratio on detectability in PET images. J Nucl Med, 41(4), 745-754,(2000).
3) Strother SC, Casey ME, and Hoffman EJ: Measuring PET scanner sensitivity: relating countrates to image signal-to-noise ratios using noise equivalents counts. IEEE Trans Nucl Sci, 37(2), 783-788,(1990).
4) Nat. Elect. Manufacturers Assoc.: NEMA Standards Publ. NU 2-2001-Performance Measurements of Positron Emission Tomographs. Rosslyn, VA,(2001).
5) Watson CC, Casey ME, Bendriem B, et al.: Optimizing injected dose in clinical PET by accurately modeling the counting-rate response functions specific to individual patient scans. J Nucl Med, 46(11), 1825-1834,(2005).
6) Spinks TJ, Miller MP, Bailey DL, et al.: The effect of activity outside the direct field of view in a 3D-only whole-body positron tomograph. Phys Med Biol, 43(4), 895-904,(1998).
7) Watson CC, Newport D, Casey ME, et al.: Evaluation of simulation-based scatter correction for 3-D PET cardiac imaging. IEEE Trans Nucl Sci, 44(1), 90-97,(1997).
8) 楠岡英雄，西村恒彦，監修：5 PET．日本エム・イー学会編　核医学イメージング．pp.118-159，コロナ社，東京，(2001).
9) Adam LE, Zaers J, Ostertag H, et al.: Performance evaluation of the whole-body PET scanner ECAT EXACT HR+ following the IEC standard. IEEE Trans Nucl Sci, 44(3), 1172-1179,(1997).
10) 日本アイソトープ協会　医学・薬学部会　サイクロトロン核医学利用専門委員会　核医工学ワーキンググループ：PET装置の性能評価のための測定指針．Radioisotopes, 43(9), 115-135, (1994).
11) Bergström M, Eriksson L, Bohm C, et al.: Correction for scattered radiation in a ring detector positron camera by integral transformation of the projections. J Comput Assist Tomogr, 7(1), 42-50,(1983).
12) 松本圭一，松浦　元，簑田英理，他：三次元全身FDG-PET収集におけるBody Mass Indexを用いた投与量および収集時間の最適化．日放技学誌，60(11)，1564-1573，(2004).
13) Defrise M, Kinahan PE, Townsend DW, et al.: Exact and approximate rebinning algorithms for 3D-PET data. IEEE Trans Med Imaging, 16(2), 145-158,(1997).
14) 松本圭一，和田康弘，松浦　元，他：PET装置におけるLine of Responseを考慮した新しい雑音等価係数指標の評価．日放技学誌，60(8)，1116-1122，(2004).
15) 山本誠一，三浦修一，飯田秀博，他：PETの3次元収集における被検体の形状と計数率特性の関係．核医学，33(4)，435-441，(1996).
16) 大西英雄，木田哲生，篠原広行，他：SPECTの再構成法に関する研究班報告．日放技学誌，59(10)，1229-1247，(2003).
17) 山田勝彦，野原弘基：第7章　計数値の統計的取扱い．日本放射線技術学会編　診療放射線技術学大系一専門技術学系13放射線計測学．pp.179-186，通商産業研究社，(1981).
18) Badawi RD, Adam L-E, and Zimmerman RE: A simulation-based assessment of the revised NEMA NU-2 70-cm long test phantom for PET. In: Nuclear Science Symposium and Medical Imaging Conference Record. San Diego: IEEE; M6-6,(2001).
19) Germano G, and Hoffman EJ: A study of data loss and mispositioning due to pileup in 2-D detectors in PET. IEEE Trans Nucl Sci, 37(2), 671-675,(1990).
20) 松本圭一，和田康弘：Positron Emission Tomographyにおける低カウント領域でのFBP法とOS-EM法の比較．核医学技術，23(3)，191-198，(2003).
21) Casey ME, and Hoffman EJ: Quantitation in positron emission computed tomography: 7. A technique to reduce noise in accidental coincidence measurements and coincidence efficiency calibration. J Comput Assist Tomogr, 10(5), 845-850,(1986).
22) Herzog H, Tellmann L, Hocke C, et al.: NEMA-NU2-2001 guided performance evaluation of four Siemens ECAT-PET scanners. IEEE Trans Nucl Sci, 51(5), 2662-2669,(2004).
23) Ferreira NC, Trebossen R, Lartizien C, et al.: A hybrid scatter correction for 3D PET based on an estimation of the distribution of unscattered coincidences: implementation on the ECAT EXACT HR+. Phys Med Biol, 47(9), 1555-1571,(2002).

図表の説明

Fig. 1　二次元収集におけるNECと放射能濃度の関係
Fig. 2　三次元収集におけるNECと放射能濃度の関係
Fig. 3　20cmϕ×20cm円筒ファントムを用いた二次元収集におけるNECと画質の関係：FBP法(a)とOSEM法(b)
直線は全画像スライスにおける回帰直線.
Fig. 4　20cmϕ×70cm円筒ファントムを用いた二次元収集におけるNECと画質の関係：FBP法(a)とOSEM法(b)
直線は全画像スライスにおける回帰直線.
Fig. 5　20cmϕ×20cm円筒ファントムを用いた三次元収集におけるNECと画質の関係：FBP法(a)とOSEM法(b)
直線は全画像スライスにおける回帰直線.
Fig. 6　20cmϕ×70cm円筒ファントムを用いた三次元収集におけるNECと画質の関係：FBP法(a)とOSEM法(b)
直線は全画像スライスにおける回帰直線.
Fig. 7　最大NECにおける二次元および三次元収集の各スライスの画質
すべての画像はFBPを用いて画像再構成を行った.

Table　(社)日本アイソトープ協会：PET装置の性能評価のための測定指針で評価されたPET装置の性能

Jpn J Clin Oncol 2007;37(8)615–622
doi:10.1093/jjco/hym064

Inter-observer Variations in FDG-PET Interpretation for Cancer Screening

Akiko Suzuki[1], Yuji Nakamoto[2], Takashi Terauchi[3], Masami Kawamoto[4], Yoshihiro Okumura[5], Yutaka Suzuki[6], Toshihiko Sato[7], Nobukazu Takahashi[8], Jin Lee[8], Michio Senda[9], Kimiichi Uno[10] and Tomio Inoue[8]

[1]Department of Radiology, School of Medicine, Yokohama City University, Yokohama, [2]Department of Diagnostic Radiology, Kyoto Graduate University School of Medicine, Kyoto, [3]Research Center for Cancer Prevention and Screening, Cancer Screening Division, National Cancer Center, Tokyo, [4]Diagnostic Imaging Center, Radiology, Yuai Clinic, Yokohama, [5]Department of Radiology, PET/RI center, Okayama Kyokuto Hospital, Okayama, [6]HIMEDIC Imaging Center at Lake Yamanaka, Yamanashi, [7]Utsunomiya Central Clinic PET Center, Utsunomiya, [8]Department of Radiology, School of Medicine, Yokohama City University, Yokohama, [9]Institute of Biomedical Research and Innovation, Kobe and [10]Nishidai Clinic Diagnostic Imaging Center, Tokyo, Japan

Received October 16, 2006; accepted March 20, 2007; published online August 18, 2007

Background: Diagnostic guidelines for the use of 2-(fluorine 18) fluoro-2 deoxy-D-glucose (FDG)-positron emission tomography (PET) in cancer screening have yet to be established. We assessed inter-observer variability in screening FDG-PET.
Methods: Subjects comprised 40 individuals who underwent FDG-PET and computed tomography (CT) for cancer screening. To assess various patterns of FDG uptakes, three subsets of the cases were selected: 'Cancer', 15 cases with cancer; 'Not malignant', 15 cases with suspected cancer by FDG-PET who were confirmed as cancer-free; and 'Normal', 10 cases without remarkable FDG uptake who were confirmed as cancer-free. A total of 68 lesions made up of malignancy ($n = 18$), benign ($n = 21$), and physiological FDG uptake ($n = 29$) were interpreted by six physicians. Each observer reviewed each case three times. Step 1 involved interpretation of PET images alone, Step 2 involved side-by-side reading of PET and CT images, and Step 3 involved re-evaluation of findings with the results of other screening tests. We assessed inter-observer agreement for each step.
Results: Inter-observer agreement for all lesions at each step was moderate, compared to fair agreement for 'Normal' subjects. Inter-observer agreement of 'Cancer' and 'Not malignant' subjects in Step 1 were better than those in Step 2 and 3; however, the differences were not statistically significant.
Conclusion: The interpretation of FDG-PET is adequately reproducible, while that of 'Normal' subjects is less reproducible. Improvement of inter-observer variability in assessing physiological FDG uptakes requires universal reporting criteria in FDG-PET. Correlative interpretation of PET, CT and other information may require standardization in subjects with suspected cancer by FDG-PET.

Key words: radiology – PET – radiology – CT/MRI – cancer screening

INTRODUCTION

2-(fluorine 18) fluoro-2 deoxy-D-glucose (FDG)-positron emission tomography (PET) plays an important role in the detection of malignant tumors, although the effectiveness of whole-body FDG-PET imaging in cancer screening remains uncertain (1,2). FDG-PET scans have been performed for cancer screening in Japan on many asymptomatic individuals who had previously never been diagnosed with cancer. FDG-PET is considered to be useful for whole-body survey because it can detect cancers of various organs that any single conventional organ-specific screening test cannot cover. High detection rates for a wide variety of cancers in cancer-screening FDG-PET has been reported by Yasuda (3)

For reprints and all correspondence: Akiko Suzuki, Department of Radiology, School of Medicine, Yokohama City University, 3–9 Fukuura, Kanazawa-ku, Yokohama, Kanagawa, 236-0004, Japan. E-mail: akiko225@yokohama-cu.ac.jp

and Chen (4); however, FDG-PET cannot be an alternative to other conventional screening tests such as physical examination, laboratory studies, mammography and thoracic computed tomography (CT), because FDG-PET analysis has obvious limitations in detecting urological cancers, cancers of low cell density, small cancers and hypometabolic or FDG-negative cancers (1,3,5). Diagnostic guidelines for the use of whole-body FDG-PET imaging in cancer screening have yet to be established. Furthermore, FDG-PET may be better interpreted with reference to CT images in cancer screening, as the determination of the precise location of FDG-avid lesions using PET alone can be challenging (6). The role of whole-body FDG-PET and CT in cancer screening is yet to be evaluated.

We surveyed a large number of cancer-screening centers in Japan in January 2005 to investigate the actual situation of cancer screening by FDG-PET. Thirty cancer-screening centers answered the questionnaire and the results were reported (data not published). The recall rate (i.e. the rate recommending diagnostic work-up due to positive findings suggesting possible cancer) varied widely from 1 to 44% betweem the centers. We hypothesized that inter-observer variation in FDG-PET interpretation for cancer screening affected clinical decisions to recommend either close examination or follow-up and caused variability in the recall rate. Inter-observer variation in FDG-PET for cancer screening is of particular interest because of the challenge involved in detecting suspected lesions, of which the incidence is very low, out of numerous cases of equivocal FDG uptake; some radiologists tend to over-diagnose FDG uptake to avoid potential false negative outcomes. Numerous investigations have shown that considerable variability exists among radiologists in the interpretation of screening tests such as mammography and thoracic CT without training or computer-aided diagnosis (7–9). This variability affects the diagnostic accuracy of screening studies and clinical decisions to recommend either close examination or follow-up. Herder et al. reported that inter-observer agreement of FDG-PET between clinical and final stage was good in patients with suspected lung cancer (10). Inter-observer agreement of interpretation in relevant focal pulmonary abnormality of FDG-PET was also reported to be good by Joshi et al. (11). To the best of our knowledge, variability in radiologists' interpretations of whole-body FDG-PET for cancer screening has yet to be examined. The purpose of the present study is to assess inter-observer variations in screening FDG-PET.

MATERIALS AND METHODS

Case Materials

FDG-PET and CT data of 40 subjects (21 male, 19 female, median age 57 years) were collected from seven cancer-screening centers in Japan and were used in this study. The scanning took place between April 2004 and March 2005; all subjects were symptom-free and underwent FDG-PET and CT on the same day for cancer screening together with other physical and laboratory tests. The 40 subjects consisted of Group 1 'Cancer', 15 true positive cases with suspected cancer by FDG-PET who were confirmed to have cancer by biopsy; Group 2 'Not malignant', 15 false positive cases with suspected cancer by FDG-PET and recommended for close examination who were confirmed as cancer-free on follow-up or biopsy; and Group 3 'Normal', 10 true negative cases who had no suspected lesion detected in FDG-PET and were confirmed to be cancer-free at 1-year follow-up. It should be noted that the number of cases in each group does not reflect the fractional occurrence of each outcome in cancer screening using FDG-PET. This study did not deal with false negative cases on PET because this is peripheral to the primary aim of assessing inter-observer variation in the interpretation of malignant lesions without remarkable FDG uptakes. Among the 15 'Cancer' subjects, primary disease involved the lung ($n = 3$), thyroid ($n = 3$), colon ($n = 2$), breast ($n = 2$), stomach ($n = 2$), pancreas ($n = 1$) and malignant lymphoma ($n = 2$). These cancers are commonly detected in FDG-PET and CT during cancer screening (1,4).

On reviewing the 40 subjects together with all the reference data, a total of 103 lesions were identified, presenting varying intensities of FDG uptake. Thirty-five of 103 lesions that were considered true negative lesions in 'Cancer' and 'Not malignant' cases were excluded because of the absence of confirmed reference data. A final total of 68 lesions were diagnosed as malignant ($n = 18$), benign ($n = 21$), or physiological FDG uptake ($n = 29$). Among the 15 'Cancer' subjects, 18 malignant lesions were detected and enrolled as true positive lesions. In the 15 'Not malignant' subjects, 13 benign lesions and five physiological uptakes were enrolled as false positive lesions. In the 10 'Normal' subjects, eight benign lesions and 24 physiological uptakes were enrolled as true negative lesions. All malignant lesions and seven benign lesions were confirmed on biopsy. At 1 year after FDG-PET, 14 benign lesions and 29 physiological uptakes were confirmed as stable or diminished in uptake. In the present study, we examine the interpretations of these 68 lesions made by each physician.

Scanning of Whole-Body PET and CT Study

FDG-PET and CT of the 40 cases were performed in seven different institutions between April 2004 and March 2005. All PET images were obtained using a standardized protocol in accordance with the FDG-PET guidelines for cancer screening issued in 2004 by the Japanese Society of Nuclear Medicine. Patients fasted for at least 5 h prior to scanning. We obtained a whole-body PET image from the head to the thigh using a PET or PET/CT scanner at 50–60 min following the injection of 300–450 MBq of FDG. Transmission images were obtained to correct for photon attenuation using a germanium-68 line source. For PET/CT, PET attenuation

correction factors were calculated from the CT images. We reconstructed image datasets using the ordered-subsets expectation maximization algorithm. We acquired a whole-body CT image from the head to the pelvis without intravenous contrast agent using a CT scanner or PET/CT scanner. The CT scanners and technical parameters were as follows: (i) Robusto (Hitachi Medico, Tokyo, Japan) multi-detector four row CT, 120 kVp, 100–160 mAs, beam pitch 1.75 and 10 mm thickness; (ii) Light Speed Ultra (GE Medical Systems, Tokyo, Japan) multi-detector eight row CT, 120 kVp, 175 mAs maximum with automatic exposure control system, 1.35 pitch and 5 mm thickness; (iii) Brilliance 16 (Philips Electronics Japan, Tokyo, Japan) multi-detector 16 row CT, 120 kVp, 150 mAs maximum with automatic exposure control system, 0.9 pitch and 5 mm thickness; (iv) Biograph LSO (Siemens-Asahi Medical Technologies, Tokyo, Japan) PET/CT with multi-detector two row CT, 130 kVp, 80 mAs maximum with automatic exposure control system, 1.15 pitch and 4 mm thickness; (v) Biograph LSO (Siemens-Asahi Medical Technologies), PET/CT with multi-detector two row CT, 130 kVp, 60 mAs, 1.5 pitch and 3 mm thickness; (vi) Eminence-SOPHIA (Shimadzu Corporation, Kyoto, Japan) helical CT, 120 kVp, 187.5 mAs, 1.4 pitch and 7 mm thickness; (vii) CT-Turbo (Hitachi Medico) helical CT, 120 kVp, 100–120 mAs, and 5–10 mm thickness. The mAs settings were selected to optimize spatial and contrast resolution. Tube current modulation was used to minimize the radiation dose to the individuals.

The PET/CT images were divided into PET and CT images, which were interpreted by side-by-side reading.

Observing Radiologists

FDG-PET and CT data were interpreted by six physicians with experience in both FDG-PET and CT, but who had not previously seen the study cases. The six observers were based at the six different cancer-screening centers with various recall rates from 1 to 44% [1, 10, 12, 23, 35, 44] that were mentioned in the introduction; each observer had between 4 and 10 years experience in reading screening FDG-PET.

Image Interpretation

Each observer reviewed each case in three steps. Step 1 involved interpretation of PET images alone, Step 2 involved side-by-side reading of PET and CT, and Step 3 involved re-evaluation of findings with reference to past history, smoking and drinking habits, and the results of other screening tests performed at the same time such as blood tests, fecal occult blood inspection and other imaging modalities that included magnetic resonance (MR) imaging for lower abdomen assessment and ultrasonography (US) for upper abdomen and thyroid gland assessment. In Step 2, each observer interpreted PET and CT by side-by-side reading without using fusion images. Findings of FDG uptake in each step were recorded as site and score depending on the likelihood of malignancy (1–5 points: 1, definitely not malignant; 2, probably not malignant; 3, equivocal; 4, probably malignant; 5, definitely malignant).

Each observer gave a score rating for every lesion that he/she considered to represent remarkable FDG uptake in each case. We analyzed each observer's interpretation of the 68 lesions that had been identified in advance as having confirmed reference data. Any of the 68 lesions that were not recognized by the observer as remarkable FDG uptake were given a score of 1 (definitely not malignant). Any lesions that were detected other than the 68 previously mentioned were excluded from analysis because of the absence of confirmed reference data.

All images were viewed with the same software using Synapse, medical imaging and information management network system, housed at the Fujifilm's demonstration showroom in Ginza, Tokyo, Japan.

Data Analyses

We assessed observer accuracy and variation using the scores given by each observer based on the relevant lesion. Sensitivity, specificity and positive predictive value (PPV) data were calculated from the interpretations of the six observers for each step. Receiver-operating characteristic (ROC) analysis was also performed as the standard method for evaluating observer accuracy, as sensitivity and specificity offer an incomplete description of accuracy and depend on the decision threshold selected by the observer to define positive diagnoses. The area under the ROC curve (Az) was used as a summary index of accuracy. Sensitivity for malignancy was calculated as the proportion of malignancies given a rating of 3–5. Specificity was defined as the fraction of benign lesions or physiological FDG uptakes for which a rating of 1–2 was reported. Inter-observer agreement in 68 lesions on the likelihood of malignancy (1–5 points) for each step was also assessed using the κ statistic.

Statistical Analysis

The Wilcoxon matched pairs signed rank sum test was applied to the sensitivity, specificity, and PPV means for each step to test for significant differences. Values of $P < 0.05$ were considered indicative of statistically significant differences. We calculated weighted κ values to describe concordance in reporting as 'slight' (0.00–0.20), 'fair' (0.21–0.40), 'moderate' (0.41–0.60), 'substantial' (0.61–0.80), or 'almost perfect' (0.81–1.00) (12,13). We conducted all analyses using MedCalc for Windows, version 7.6.0.0 (MedCalc Software, Mariakerke, Belgium), except for ROC analysis, which was performed using the software ROCKIT (C. Metz, University of Chicago, Chicago, IL, USA). ROC software was used to fit a binormal ROC curve

to the data from each observer and to compare Az for each pair using a univariate z-score test (14).

RESULTS

Diagnostic Accuracy of Each Observer

A summary of ROC curves obtained from interpretation in Step 1 using PET alone is shown in Fig. 1. Az values did not differ significantly between the six observers for each step. The means and dispersion of sensitivity, specificity, PPV and Az are shown in Table 1. Although Az values did not differ significantly, sensitivity, specificity and PPV varied widely between the observers.

Effect of Reference to CT on Diagnostic Accuracy

The mean specificity increased significantly when observers referred to CT ($P < 0.05$), although sensitivity, PPV and Az did not change significantly (Table 1).

Variability in Interpretation

The mean κ value and the strength of inter-observer agreement for each step are shown in Table 2. Inter-observer agreement for all lesions in each step was moderate ($\kappa = 0.58$ for Step 1; $\kappa = 0.55$ for Step 2; and $\kappa = 0.53$ for Step 3).

Inter-observer agreement was higher for 'Cancer' and 'Not malignant' lesions than for 'Normal' lesions for each step (moderate versus fair).

Although the κ values for each group in Step 1 were higher than those in Steps 2 and 3, the differences were not statistically significant. The κ values of 'Cancer' and 'Not malignant' lesions in Step 2 were higher than those in Step 3; however, the differences were not statistically significant.

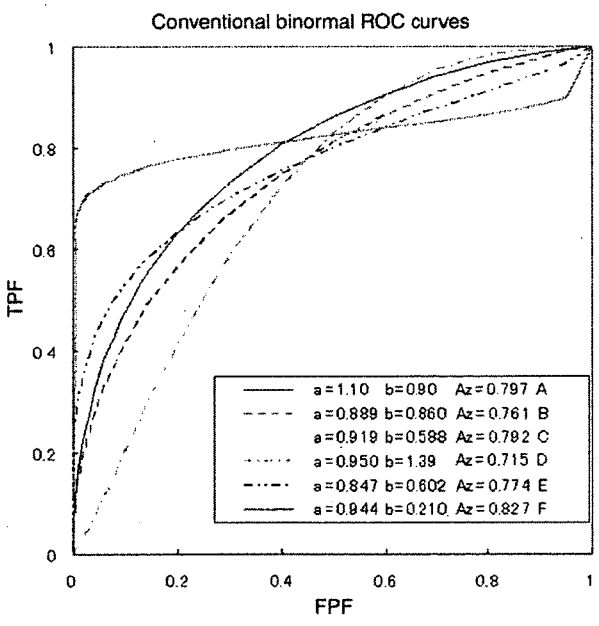

Figure 1. Summary receiver-operating characteristic curves obtained from interpretation in Step 1 of evaluations with positron emission tomography alone (please note that a colour version of this figure is available as supplementary data at http://www.jjco.oxfordjournals.org). TPF, true positive fraction; FPF, false positive fraction.

Patterns of FDG Uptake with Poor Agreement

In assessing inter-observer agreement for each organ, we determined the organs that were interpreted with difficultly by PET alone. The numbers of sites presenting poor or good agreement in each organ for the 68 lesions in Step 1 using PET alone are shown in Tables 3–5. Lesions for which fewer than five observers agreed in diagnosis were considered as poor agreement, while lesions for which five or six observers agreed in diagnosis were considered as good agreement.

FDG uptakes in the 'Normal' 32 true negative lesions that presented poor agreement included nine physiological uptakes in the larynx, mediastinum, intestine and ovary, and four benign lesions in the thyroid, neck, lung and uterus (Table 3). The case with physiological FDG uptake in the ascending colon is shown in Fig. 2.

FDG uptakes in the 18 'Cancer' true positive lesions that presented poor agreement included 10 malignant lesions in the thyroid, hilum, breast, colon and stomach (Table 4).

FDG uptakes in the 18 'Not malignant' false negative lesions that presented poor agreement included eight benign lesions in the thyroid, lung, colon and joint, and four physiological uptakes in the hilum, intestine and ovary (Table 5).

DISCUSSION

Diagnostic Accuracy of Each Observer

We assessed observer accuracy using the scores representing a rating on the likelihood of malignancy for 68 lesions by each observer. No significant differences were identified for any step in Az of the six observers. Wide variation in sensitivity, specificity and PPV detected between observers was caused by differing decision thresholds during interpretation. Selection of different thresholds does not cause Az to vary, as an ROC curve depicts all of the tradeoffs available as the threshold is varied. Therefore, variability of the decision threshold between observers exists where no significant differences were identified in diagnostic accuracy as quantified with Az. That is, the scores given for each lesion could vary between the six observers even though there were no significant differences in diagnostic accuracy indicated by Az.

Table 1. Mean (range of six observers) sensitivity, specificity, PPV and Az of FDG-PET cancer screening based on lesions

	Step 1	Step 2	Step 3
	PET alone	PET + CT	PET + CT + Other information
Sensitivity	78.7 (72.2–83.3)	75.9 (66.7–83.3)	72.2 (61.1–83.3)
Specificity	64.7* (58.0–74.0)	71.3* (64.0–78.0)	74.0* (66.0–82.0)
PPV	44.9 (41.7–51.9)	49.2 (41.9–57.7)	50.6 (39.3–60.9)
Az**	0.778 (0.715–0.827)	0.788 (0.718–0.851)	0.794 (0.704–0.848)

PET, positron emission tomography; CT, computed tomography; PPV, positive predictive value.
*Mean specificity of PET + CT and PET + CT + Other information was higher than that of PET alone (Wilcoxon matched pairs signed rank sum test, $P < 0.05$).
**Az, area under curve in ROC.

Table 2. Mean κ value and strength of inter-observer agreement for the likelihood of malignancy of 68 FDG-avid lesions in 40 cases

		Step 1	Step 2	Step 3
		PET alone	PET + CT	PET + CT + Other information
Total lesions ($n = 68$)	κ	0.58	0.55	0.53
	Agreement	Moderate	Moderate	Moderate
'Normal' ($n = 32$)	κ	0.30	0.28	0.28
	Agreement	Fair	Fair	Fair
'Cancer' ($n = 18$)	κ	0.57	0.44	0.42
	Agreement	Moderate	Moderate	Moderate
'Not malignant' ($n = 18$)	κ	0.51	0.46	0.41
	Agreement	Moderate	Moderate	Moderate

FDG, 2-(fluorine 18) fluoro-2 deoxy-D-glucose.
κ value <0, poor; 0–0.20, slight; 0.21–0.40, fair; 0.41–0.60, moderate; 0.61–0.80, substantial; 0.81–1.00, almost perfect.
'Normal': 32 true negative lesions that were not suspected malignant in FDG-PET cancer screening and were confirmed as physiological uptakes or benign lesions after 1 year.
'Cancer': 18 true positive lesions that were suspected malignant in FDG-PET screening and were later diagnosed as malignant lesions.
'Not malignant': 18 false positive lesions that were suspected malignant in FDG-PET screening and were later diagnosed as benign lesions or physiological uptakes.

Effect of Reference to CT on Diagnostic Accuracy

We defined sensitivity as the proportion of malignancies given a rating of 3–5 and specificity as the fraction of benign lesions or physiological FDG uptakes given a rating of 1–2. This classification has critical meaning, therefore, Az has less value when comparing test performance between Steps 1 to 3. The mean specificity increased significantly in this study when observers referred to CT. Chen et al. also reported that additional CT for localization and lesion characterization showed an increased specificity of PET for cancer screening in asymptomatic individuals (4). In the present study, however, mean sensitivity and PPV did not change significantly when observers referred to CT. Several investigators report that the combination of FDG-PET and CT significantly improves diagnostic accuracy in the diagnosis of malignancy (15–17). The fact that the present results demonstrate no improvement in sensitivity and PPV may be due to selection bias: the present study did not include false negative lesions of PET that are recognized in CT. Sensitivity on general FDG-PET screening may be improved when observers refer to CT, given the inclusion of CT positive lesions that are without remarkable FDG uptakes such as bronchioloalveolar lung carcinoma (18).

Variability in Interpretation

We assessed inter-observer agreement on the scores for likelihood of malignancy (1–5 points) in 68 lesions. The 68 lesions that presented varying intensities of FDG uptake were founded in whole-body FDG-PET performed for cancer screening of 40 asymptomatic individuals.

Inter-observer agreement for all lesions in each step was moderate. Berg et al. reported that inter-observer agreement

Table 3. Agreement in each site of 'Normal' 32 true negative lesions in Step 1 using PET alone

Sites	Diagnosis	No. of sites	No. of each agreement	
			Poor**	Good***
Larynx	Physiological*	2	2	0
Oral cavity	Physiological	4	0	4
Mediastinum	Physiological	2	1	1
Epigastrium	Physiological	5	0	5
Intestine	Physiological	6	4	2
Ovary	Physiological	1	1	0
Uterus	Physiological	1	0	1
Prostate	Physiological	2	0	2
Ureter	Physiological	1	0	1
Thyroid	Thyroadenitis	1	1	0
Neck	Lymphadenopathy	1	1	0
Lung	Pneumonia	2	1	1
Rib	Fracture	1	0	1
Shoulder	Arthritis	1	0	1
Liver	Cyst	1	0	1
Uterus	Myoma	1	1	0
Total		32	12	20

*Physiological: physiological FDG uptake.
**Poor: fewer than five observers agreed in diagnosis.
***Good: five or six observers agreed in diagnosis.

Table 4. Agreement in each site of the 18 'Cancer' true positive lesions in Step 1 using PET alone

Sites	Diagnosis	No. of sites	No. of each agreement	
			Poor	Good
Thyroid	Thyroid Cancer	3	3	0
Lung	Lung Cancer	2	0	2
Hilum	LN metastasis or lung cancer	2	2	0
Breast	Breast cancer	2	1	1
Colon	Colon cancer	2	2	0
Stomach	Gastric cancer	2	2	0
Pancreas	Pancreas cancer	1	0	1
Subclavicular	Lymphoma	1	0	1
Mediastinum	Lymphoma	1	0	1
Paraaorta	Lymphoma	1	0	1
Mesenterium	Lymphoma	1	0	1
Total		18	10	8

LN metastasis, lymph node metastasis.

among radiologists on mammogram screening after training in Breast Imaging Reporting and Data System was moderate (9). Our results suggest that interpretation of FDG-PET in cancer screening is adequately reproducible as a whole.

Inter-observer agreement for all lesions at each step was moderate, compared to fair agreement for 'Normal' subjects. The higher prevalence of malignant lesions (18/68) means that the set used in this study was not strictly representative of FDG-PET within the general screening population. Inter-observer agreement on general FDG-PET screening might normally be lower, given the inclusion of a larger number of normal healthy subjects. Low inter-observer agreement may cause the marked variability in recall rate among the institutions that perform screening FDG-PET.

Inter-observer agreement was lower for 'Normal' lesions than for 'Cancer' and 'Not malignant' lesions for each step (fair versus moderate). Since sensitivity are calculated based on the data for 'Cancer' and specificity are based on those for 'Not malignant' and 'Normal', inter-observer variation observed for 'Cancer' and 'Not malignant and Normal' are corresponding to variability in sensitivity and specificity between observers (58.0–74.0, 72.2–83.3 in Step 1, respectively).

Inter-observer agreement decreased when observers referred to CT, however, the differences were not statistically

Table 5. Agreement in each site of the 18 'Not malignant' false positive lesions in Step 1 using PET alone

Sites	Diagnosis	No. of sites	No. of each agreement	
			Poor	Good
Thyroid	Goiter or thyroadenitis	3	2	1
Parotid gland	Warthin tumor	1	0	1
Lung	Pneumonia or pleural tumor	4	2	2
Sternoclavicular joint	Arthritis	1	1	0
Colon	Adenoma or polyp	4	3	1
Hilum	Physiological	1	1	0
Intestine	Physiological	1	1	0
Stomach	Physiological	1	0	1
Ovary	Physiological	2	2	0
Total		18	12	6

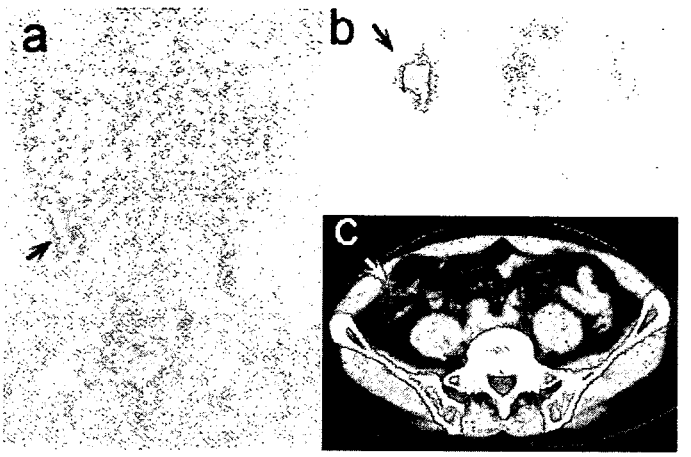

Figure 2. Physiological 2-(fluorine 18) fluoro-2 deoxy-D-glucose uptake in the intestine of 'Normal' subjects that presented poor agreement: a 54-year-old male. (a) Coronal and (b) transaxial FDG-PET image revealed focal uptake in the ascending colon (arrow). (c) The corresponding lesion was not demonstrated on CT. CT, computed tomography.

significant. Although side-by-side reading of PET and CT improves lesion localization and supports lesion characterization, correlative interpretation of PET and CT differed between observers. Metser et al. concluded that in-line PET/CT offers better lesion localization relative to visual fusion of PET and CT, especially for small lymph nodes, lesions adjacent to mobile organs and lesions adjacent to the chest or abdominal wall (19). Syed et al. reported that PET/CT increases inter-observer agreement and confidence in disease localization of FDG-avid lesions in patients with head and neck cancers (20). By precisely localizing FDG uptakes, interpretation of image fusion by integrated PET/CT might offer higher inter-observer agreement in comparison to interpretation of PET images alone or side-by-side interpretation of PET and CT images.

Although inter-observer agreement of 'Cancer' and 'Not malignant' lesions decreased when observers referred to other information, the differences were not statistically significant. In cancer screening, positive lesions are eventually recommended for diagnostic work-up or observation with close follow-up. The clinical recommendation is determined by evaluation of the PET and CT findings with reference to past history, smoking and drinking habits, and results of other screening tests. Correlative interpretation of PET, CT and other information may need to be standardized to achieve greater agreement in subjects with suspected cancer by FDG-PET.

Patterns of FDG Uptake with Poor Agreement

We evaluated the organs that were most difficult to interpret by PET alone. Some observers tended to over-diagnose FDG uptake to avoid potential false negative outcome, while others did not pick up suspected lesions in 'Normal' subjects. Physiological FDG uptake is recognized at various sites in various degrees. A focal intense uptake in intestine mimics FDG uptake of colon tumor as shown in Fig. 1. Reporting criteria for various patterns of FDG uptakes in intestine differed between observers. For higher agreement on results for the 'Normal' 32 true negative lesions in FDG-PET, interpretation of physiological FDG uptake for the larynx, mediastinum, intestine and ovary should be standardized.

Various FDG uptakes in goiter, pneumonia, colon adenoma and arthritis confound image interpretation of FDG-PET and act to reduce inter-observer agreement. Interpretation of FDG-avid lesions in the thyroid, lung, hilum, breast, colon, stomach and ovary may require standardization for higher agreement in 'Cancer' and 'Not malignant' subjects.

CONCLUSIONS

Our results suggest that interpretation of FDG-PET in cancer screening is adequately reproducible, whereas interpretation of physiological FDG uptake in 'Normal' subjects is less reproducible. Improvement of inter-observer variability in assessing physiological FDG uptakes requires universal reporting criteria in FDG-PET. Furthermore, correlative interpretation of PET, CT and other information may require standardization in subjects with suspected cancer by FDG-PET.

Acknowledgments

This research was supported in part by a Grant from Foundation for Promotion of Cancer Research and by a Health and Labor Sciences Research Grant for the project titled 'Third Term Comprehensive Control Research for Cancer' from the Ministry of Health, Labor, and Welfare, Japan.

Conflict of interest statement
None declared.

References

1. Yasuda S, Ide M. PET and cancer screening. *Ann Nucl Med* 2005;19:167–77.
2. Kubota K. From tumor biology to clinical PET: a review of positron emission tomography (PET) in oncology. *Ann Nucl Med* 2001;15:471–86.
3. Yasuda S, Ide M, Fujii H, Nakahara T, Mochizuki Y, Takahashi W, et al. Application of positron emission tomography imaging to cancer screening. *Br J Cancer* 2000;83:1607–11.
4. Chen YK, Ding HJ, Su CT, Shen YY, Chen LK, Liao AC, et al. Application of PET and PET/CT imaging for cancer screening. *Anticancer Res* 2004;24:4103–8.
5. Nakai K, Yasuda S, Ide M, Kawada S, Shohtsu A. Cancer screening with 18F FDG-PET. In: Oeher P, Biersack HJ, Coleman RE editors. *PET and PET-CT in Oncology*. Heidelberg: Springer 2004; 309–20.
6. Ak I, Stokkel MP, Pauwels EK. Positron emission tomography with 2-(18F) fluoro-2-deoxy-D-glucose in oncology. Part II. The clinical value in detecting and staging primary tumours. *J Cancer Res Clin Oncol* 2000;126:560–74.
7. Jiang Y, Nishikawa RM, Schmidt RA, Toledano AY, Doi K. Potential of computer-aided diagnosis to reduce variability in radiologists' interpretations of mammograms depicting microcalcifications. *Radiology* 2001;220:787–94.
8. Rubin GD, Lyo JK, Paik DS, Sherbondy AJ, Chow LC, Leung AN, et al. Pulmonary nodules on multi-detector row CT scans: performance comparison of radiologists and computer-aided detection. *Radiology* 2005;234:274–83.
9. Berg WA, D'Orsi CJ, Jackson VP, Bassett LW, Beam CA, Lewis RS, et al. Does training in the Breast Imaging Reporting and Data System (BI-RADS) improve biopsy recommendations or feature analysis agreement with experienced breast imagers at mammography? *Radiology* 2002;224:871–80.
10. Herder GJ, Kramer H, Hoekstra OS, Smit EF, Pruim J, van Tinteren H, et al. Traditional versus up-front (18F) fluorodeoxyglucose-positron emission tomography staging of non-small-cell lung cancer: a Dutch cooperative randomized study. *J Clin Oncol* 2006;24:1800–6.
11. Joshi U, Raijmakers PG, van Lingen A, Comans EF, Pijpers R, Teule GJ, et al. Evaluation of pulmonary nodules: comparison of a prototype dual crystal (LSO/NAI) dual head coincidence camera and full ring positron emission tomography (PET). *Eur J Radiol* 2005;55:250–4.
12. Kundel HL, Polansky M. Measurement of observer agreement. *Radiology* 2003;228:303–8.
13. Landis JR, Koch GG. The measurement of observer agreement for categorical data. *Biometrics* 1977;33:159–74.
14. Metz CE. Some practical issues of experimental design and data analysis in radiological ROC studies. *Invest Radiol* 1989;24:234–45.
15. Eubank WB, Mankoff DA, Schmiedl UP, Winter TC, III, Fisher ER, Olshen AB, et al. Imaging of oncologic patients: benefit of combined CT and FDG PET in the diagnosis of malignancy. *Am J Roentgenol* 1998;171:1103–10.
16. Aquino SL, Asmuth JC, Alpert NM, Halpern EF, Fischman AJ. Improved radiologic staging of lung cancer with 2-(18F)-fluoro-2-deoxy-D-glucose-positron emission tomography and computed tomography registration. *J Comput Assist Tomogr* 2003;27:479–84.
17. Yoshida Y, Kurokawa T, Kawahara K, Tsuchida T, Okazawa H, Fujibayashi Y, et al. Incremental benefits of FDG positron emission tomography over CT alone for the preoperative staging of ovarian cancer. *Am J Roentgenol* 2004;182:227–33.
18. Higashi K, Ueda Y, Seki H, Yuasa K, Oguchi M, Noguchi T, et al. Fluorine-18-FDG PET imaging is negative in bronchioloalveolar lung carcinoma. *J Nucl Med* 1998;39:1016–20.
19. Metser U, Golan O, Levine CD, Even-Sapir E. Tumor lesion detection: when is integrated positron emission tomography/computed tomography more accurate than side-by-side interpretation of positron emission tomography and computed tomography? *J Comput Assist Tomogr* 2005;29:554–9.
20. Syed R, Bomanji JB, Nagabhushan N, Hughes S, Kayani I, Groves A, et al. Impact of combined (18)F-FDG PET/CT in head and neck tumours. *Br J Cancer* 2005;92:1046–50.

ELSEVIER

NeuroImage

www.elsevier.com/locate/ynimg
NeuroImage 24 (2005) 70–81

Orthostatic posture affects brain hemodynamics and metabolism in cerebrovascular disease patients with and without coronary artery disease: a positron emission tomography study

Yasuomi Ouchi,[a,b,*] Etsuji Yoshikawa,[c] Toshihiko Kanno,[a] Masami Futatsubashi,[c] Yoshimoto Sekine,[a,c] Hiroyuki Okada,[c] Tatsuo Torizuka,[a] and Keisei Tanaka[d]

[a]*Positron Medical Center, Hamamatsu Medical Center, Hamakita, Japan*
[b]*Department of Neurology, Hamamatsu Medical Center, Hamamatsu, Japan*
[c]*Central Research Laboratory, Hamamatsu Photonics K.K., Hamakita, Japan*
[d]*Department of Neurosurgery, Hamamatsu Medical Center, Hamamatsu, Japan*

Received 27 January 2004; revised 8 July 2004; accepted 12 July 2004
Available online 11 November 2004

To investigate whether a physiological change in the orthostatic condition is associated with a deterioration of cerebrovascular and metabolic homeostasis in patients with neurocardiovascular compromises, we examined 10 patients with unilateral carotid artery occlusive disease (CVD), 6 CVD patients with coronary artery disease (CVDC), and 10 healthy subjects scanned twice under supine and sitting conditions by positron emission tomography (PET). Repeated measures analysis of variance showed significant reductions in regional cerebral blood flow (rCBF) and cerebral oxygen metabolism ($rCMRO_2$) and tendency of increase in oxygen extraction fraction (OEF) in the affected-side parietal cortex during assuming of upright posture in the CVDC group, and there was a significant OEF increase to maintain $rCMRO_2$ constant during sitting in the CVD counterpart. In this ischemic region, there were negative correlations between changes in OEF and rCBF in the CVD ($P < 0.05$) and CVDC groups ($P < 0.01$). Postural reductions in rCBF and CMRO2 in the parietal region were significantly greater in the CVDC group than those in the CVD group. While rCBF remained constant with mean arterial blood pressure (MABP) in healthy subjects, an rCBF reduction was found in the affected parietal cortex in proportion to the upright posture-induced MABP decrease in the CVDC group. These results indicate that patients suffering from both cerebral and coronary artery diseases may be at greater risk of deterioration of local perfusion pressure and metabolic regulation in the hemodynamically susceptible brain region during upright posture.

Keywords: Cerebral artery occlusion; Upright posture; Cerebral oxygen metabolism; Cerebral blood flow; Positron emission tomography

Introduction

It is widely accepted that a sudden reduction in blood pressure can affect cerebral blood flow (CBF) and render an elderly subject vulnerable to orthostatic symptoms such as dizziness, falls, or syncope (Graafmans et al., 1996; Lipsitz, 1989). A prolonged upright posture could trigger syncope even in healthy subjects, due chiefly to neurally mediated (vasovagal) fainting (Kapoor, 2000), and in patients with coronary artery disease, due to impairments in blood pressure regulation (Pitzalis et al., 2002). Therapeutically, it has been reported that in healthy subjects, drinking a substantial amount of water helps prevent deterioration of CBF regulation during the head-up tilt condition (Schroeder et al., 2002). These findings suggest that an orthostatic physiological change during head-up posture would be more dangerous to stroke patients, because their ischemic brain regions are likely susceptible to local hypoperfusion changes during sitting (Ouchi et al., 2001a). Thus, it is expected that not only CBF, but also metabolic regulation, would vary dynamically while human subjects are in an upright posture, especially those patients with hemodynamically compromised cerebrocardiovascular circulation, for example, major cerebral artery occlusion with coronary artery stenosis.

Many investigators have so far reported reductions in large vessel flow velocity (Levine et al., 1994; Schondorf et al., 1997) and CBF in the distal part of the internal carotid artery domain (Hayashida et al., 1993; Ouchi et al., 2001a; Warkentin et al., 1992), occasionally along with a reduction in oxygen supply to the region (Mehagnoul-Schipper et al., 2000) during assumption of an upright posture. An orthostatic change of blood pressure may be a major contributor to cerebral ischemic stroke, because the magnitude of postural hypotension could be an index for cerebrovascular mortality rates (Raiha et al., 1995), and because reduced circadian blood pressure could trigger

* Corresponding author. Positron Medical Center, Hamamatsu Medical Center, 5000 Hirakuchi, Hamakita 434-0041, Japan. Fax: +81 53 585 0367.
E-mail address: ouchi@pmc.hmedc.or.jp (Y. Ouchi).
Available online on ScienceDirect (www.sciencedirect.com.)

1053-8119/$ - see front matter © 2004 Elsevier Inc. All rights reserved.
doi:10.1016/j.neuroimage.2004.07.044

further ischemic insults in poststroke patients (Lakka et al., 1999; Strandgaard and Paulson, 1989). Animal experiments have shown that when the systemic blood pressure decreases below the lower limit of cerebral autoregulation, multiple ischemic loci are generated (Hamar et al., 1979), and a reduction in the cerebral arteriolar pressure in the ischemic region distal to an arterial occlusion occurs (Paulson, 1970; Symon et al., 1976). The same theory could be applied to patients with internal carotid artery occlusive disease (ICAO), because there is a gradual decrease in regional cerebral blood flow (rCBF) together with an elevation in the oxygen extraction fraction (OEF) in an axial-direction fashion on the occlusion side (Yamauchi et al., 1990).

The purpose of the present study was to investigate, using positron emission tomography (PET), absolute changes in rCBF and oxygen metabolism in cerebrovascular patients with and without coronary artery disease during assumption of an upright posture in order to elucidate the orthostatic deterioration in hemodynamic and metabolic regulations in the hemodynamically vulnerable brain region.

Subjects and methods

Patients

The patient groups consisted of only patients with an occlusion or 99% stenosis in the unilateral ICA. Sixteen patients (11 men and 5 women) with cerebrovascular disease and 10 healthy volunteers (5 men and 5 women, 58.7 ± 6.7 years) participated. The patients were divided into two groups according to the comorbidity of clinically stable coronary artery disease (occlusion or stenosis); a group without cardiac problems (carotid artery occlusive disease (CVD) group; n = 10, 6 men and 4 women, mean ± SD, 65.1 ± 7.3 years) and a group with cardiac ischemia (coronary artery disease (CVDC) group; n = 6, 5 men and 1 woman, 64.2 ± 9.5 year). The third group (normal group) consisted of the 10 healthy volunteers. No significant difference was found in age among the three groups (t test, $P > 0.05$). The clinical characteristics of each patient are summarized in Table 1. Electrocardiogram showed a typical ST-segment depression in all CVDC patients and a small change of ST segment and T wave in

Table 1
Patient characteristics

No	Age	Sex	Diagnosis	Side	DD	Symptoms	Complications	HIAs on T2-MRI	AG	ECG	Medication
CVD											
1	53	M	ICAS	R	0.2	NS, Sensory disturbance	DM	subCx WM	BZ	normal	anti-DM
2	71	M	ICAO	L	0.5	R hemiparesis	None	L basal ganglia	BZ	normal	None
3	68	M	ICAS	R, L	0.4	L hemiparesis	HT	LR hemispheric subCx WM	PC	normal	anti-HT, anti-coag
4	57	M	ICAS	L, R	1.5	Tinnitus, TIA	HT	L frontal subCx WM	BZ	normal	anti-HT, anti-HMG
5	71	M	ICAO	R	0.3	Dysphagia, Dysphasia	None	LR hemispheric subCx WM	BZ	normal	anti-coag
6	72	M	ICAO	R	0.2	L weakness, impaired gait	None	R watershed subCx WM	BZ	normal	anti-coag
7	71	F	ICAO, ICAS	L, R	0.8	TIA (R motor weakness)	HT	L hemispheric subCx WM	PC	ST	anti-HT, anti-coag
8	69	F	ICAS	L	1.5	Mild apraxia	HT	R, L basal ganglia	CC, BZ	normal	anti-HT, anti-coag
9	56	F	ICAO	R	0.2	TIA (L motor weakness)	None	subCx WM	BZ	normal	anti-coag
10	63	F	ICAO	L	1.2	Tinnitus	None	subCx WM	BZ	normal	None
CVDC											
1	60	M	ICAOc	L	1.1	TIA (R motor weakness),	HT, HU, AP,	subCx WM	PC	ST	anti-HT, anti-AP, anti-HU
2	76	M	ICASc	L	0.4	Faintness, collapse,	MI, Ar	L hemispheric subCx WM	BZ	ST	anti-coag, anti-AP
3	53	M	ICASc	R	0.5	TIA (L motor weakness)	DM, AP	subCx WM	BZ	ST	anti-DM, anti-AP
4	55	F	ICAOc	L	0.3	Aphasia, TIA	HC, AP, Ar	L hemispheric subCx WM	PC	ST	anti-coag, anti-HC, anti-AP
5	72	M	ICAOc, ICASc	L, R	1.0	R, L hemiparesis	HT, AP	R, L subCx WM	BZ	ST	anti-HT, anti-AP
6	69	M	ICAOc	R	0.2	Dysartheia, Paraparesis	HT, AP	R, L subCx WM, pons	CC, BZ	ST	anti-HT, anti-AP

ICAO, internal carotid artery occlusion; ICAS, internal carotid artery stenosis; ICAOc, internal carotid artery occlusion with coronary artery disease; DD, disease duration from onset to PET measurement (years); TIA, transient ischemic attack; HIAs, high intensity areas; ECG, electrocardiogram; ST, ST-segment depression and T wave changes; Cx, cortex; subCx, subcortex; WM, white matter; AG, angiography; BZ, border zone shift; CC, cross circulation; PC, pial collateralization to the insula level; HT, hypertension; DM, diabetes mellitus; HU, hyperuricemia; AP, angina pectoris; MI, myocardial infarction; HC, hypercholesteremia; Ar, arrhythmia; R, right; L, left; anti-HT, anti-hypertensive drug; anti-HMG, 3-hydroxy-3methylglutaryl-coenzyme A (HMG-CoA) reductase inhibitor for treatment of hypercholesterolemia; anti-DM, oral drug for Diabetes mellitus; anti-coag, anticoagulant drug.